Journal of Solid State Chemistry 181 (2008) 3217–3222

Contents lists available at ScienceDirect

Journal of Solid State Chemistry

journal homepage: www.elsevier.com/locate/jssc

Synthesis, physicochemical characterization and crystallographic twinning of Li_2ZnSnS_4

Jonathan W. Lekse [a], Beth M. Leverett [b], Charles H. Lake [b], Jennifer A. Aitken [a,*]

[a] Department of Chemistry and Biochemistry, Duquesne University, 600 Forbes Avenue, Mellon Hall 302, Pittsburgh, PA 15282, USA
[b] Department of Chemistry, Indiana University of Pennsylvania, 975 Oakland Avenue, Indiana, PA 15705, USA

ARTICLE INFO

Article history:
Received 13 June 2008
Received in revised form
8 August 2008
Accepted 19 August 2008
Available online 2 September 2008

Keywords:
Semiconductor
Diamond-like
Twin
Thiostannate
Wurtz-stannite

ABSTRACT

Li_2ZnSnS_4 is a new diamond-like semiconductor, which is of interest as a host structure for the creation of potentially interesting electronic, magnetic and photovoltaic materials. The compound was synthesized via traditional high-temperature solid-state methods and was predicted to adopt a wurtz-stannite structure with all atoms possessing tetrahedral environments. Initial analysis of single-crystal X-ray diffraction data indicated crystallographic disorder that upon closer examination violated basic chemical principles. The structure was subsequently re-evaluated and the apparent "disorder" problem was found to be the result of pseudo-merohedral twinning. The crystal structure was finally solved in the monoclinic space group *Pn*, which resulted in a chemically reasonable model. The refinement converged with $R1 = 1.68\%$ (for all data). Additional characterization of the sample, including diffuse reflectance, thermal analysis and second harmonic generation measurements, was also performed.

1. Introduction

Diamond-like semiconductors (DLS) are normal valence compounds, which are homeotypes of the crystal structure of diamond [1–5]. These compounds are technologically useful and have been investigated for a variety of applications including photovoltaics [6], nonlinear optics [7,8], thermoelectrics [9] and spintronics [10]. In order to be considered a diamond-like semiconductor, a compound must obey a number of criteria. First, the average number of valence electrons must equal four and the number of valence electrons per anion must equal eight. Additionally, all atoms must possess tetrahedral environments and obey Pauling's electrostatic valency rule, which states that the valence of each anion must be satisfied by the valence of the cations in its immediate coordination sphere. The number of compounds that satisfy these criteria is finite, but not insubstantial. To date, a large volume of research has been conducted on binary and ternary DLS; however, related quaternary DLS [3–5] have not attracted as much interest. Quaternary DLS should possess similar properties and the possibility of physical property tuning should increase as the degree of cationic substitution increases. The progression of diamond-like homeotypes from binary to quaternary using three known compounds, ZnS [11,12], $AgInS_2$ [13] and Cu_2CdGeS_4 [3], can be found in Fig. 1.

Quaternary DLS possess a number of structural features that can result in interesting physical properties. Pauling's electrostatic valency principle predicts that each sulfide anion can only be bound to one divalent cation, two univalent cations and one tetravalent cation. This should be important when using these systems as host materials for dilute magnetic semiconductors, as the divalent cations are significantly further apart than those found in the binary DLS materials and can be separated by low-electron-density, univalent cations, such as lithium.

In this work, the synthesis and characterization of the quaternary DLS, Li_2ZnSnS_4, will be described. This will include a detailed discussion of how a structure that was initially thought to possess crystallographic disorder was determined to be a pseudo-merohedral twin, using a combination of chemical and crystallographic principles.

2. Experimental

2.1. Reagents

Chemicals in this work were used as obtained: (1) lithium sulfide (Li_2S) powder, −200 mesh, 99.9%, Cerac; (2) zinc powder, −140+325 mesh, 99.9%, Cerac; (3) tin powder, −100 mesh, 99.999%, Strem; and (4) sulfur powder, sublimed, 99.5%, Fisher.

* Corresponding author. Fax: +1 412 396 5683.
E-mail address: aitkenj@duq.edu (J.A. Aitken).

0022-4596/$ - see front matter © 2008 Elsevier Inc. All rights reserved.
doi:10.1016/j.jssc.2008.08.026

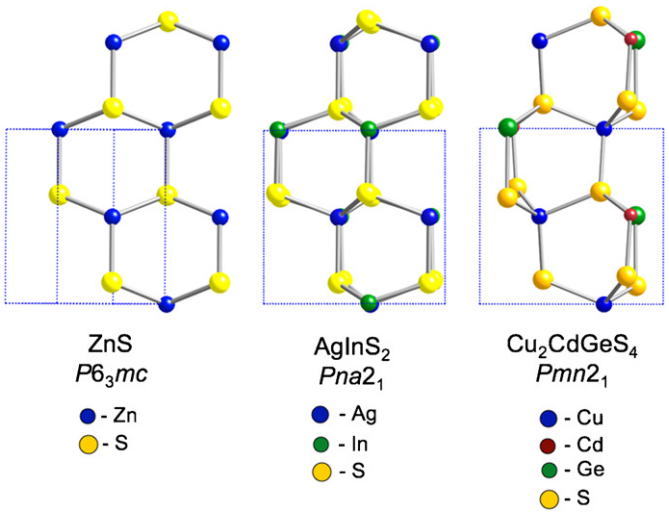

Fig. 1. The structural progression from binary to quaternary diamond-like semiconductors with hcp is illustrated by three compounds. A similar progression can be derived from cubic diamond (ccp).

2.2. Synthetic procedure

2.2.1. Li_2ZnSnS_4 powder

1 mmol of Li_2ZnSnS_4 was prepared by weighing and grinding Li_2S (1.2 mmol), Zn (1 mmol), Sn (1 mmol), and S (3 mmol) using an agate mortar and pestle in an argon-filled glovebox. The ground mixture was placed into a graphite crucible inside a 12 mm o.d. fused-silica tube. The tube was sealed under a vacuum of approximately 10^{-3} mbar, heated to 700 °C in 12 h and then held at 700 °C for 96 h. The sample was then slowly cooled to room temperature in 12 h. The graphite crucible is necessary to prevent lithium from reacting with the fused-silica. The tube was opened under ambient conditions and the contents were examined using a light microscope. A yellow-green, microcrystalline powder was obtained and used for property measurements.

2.2.2. Li_2ZnSnS_4 crystals

Stoichiometric amounts of Li_2S, Zn, Sn and S to prepare 1 mmol of Li_2ZnSnS_4 were weighed and ground in an argon-filled glovebox. The ground mixture was placed into a graphite crucible inside a 12 mm o.d. fused-silica tube. The tube was sealed under a vacuum of approximately 10^{-3} mbar, heated to 825 °C in 9 h and then held at 825 °C for 72 h. The sample was cooled slowly to 500 °C in 32.5 h and then rapidly to room temperature in 3 h. The tube was opened under ambient conditions and the contents were examined using a light microscope. Yellow-green, trapezoidal plate, X-ray-quality single crystals of the product were obtained and used for structure determination.

2.3. Physical property measurements

2.3.1. Scanning electron microscopy and energy dispersive spectroscopy (EDS)

A CamScan Series 4 scanning electron microscope was used to image samples and a Princeton Gamma Tech detector was used for EDS. The working distance was 35 mm and the accelerating voltage was set to 22.5 kV. Samples were mounted onto a double-sided carbon tape, which was adhered to an aluminum specimen holder. EDS data were collected for 60 s. The presence of zinc, tin and sulfur in each of the yellow-green crystals was confirmed, though the presence of lithium cannot be determined by this technique. Elemental mapping confirmed that each element was dispersed evenly throughout the crystals.

2.3.2. Differential thermal analysis (DTA)

DTA was performed using a Shimadzu DTA-50 thermal analyzer calibrated with a three-point calibration curve using indium, zinc and gold. The reference, Al_2O_3, and sample, of comparable masses, were contained in fused-silica ampoules (carbon coated for the sample) and sealed under a vacuum of $\sim 10^{-3}$ mbar. The temperature was programmed to increase at a rate of 10 °C/min from 25 to 1000 °C. The temperature was then decreased to 100 °C at 10 °C/min. To distinguish reversible events from irreversible ones, a second cycle was performed in the same manner.

2.3.3. Diffuse reflectance UV/Vis/NIR spectroscopy

Optical diffuse reflectance spectra were obtained using a Cary 5000 UV/Vis/NIR spectrometer. Samples were ground and loaded into a Harrick Praying Mantis diffuse reflectance accessory that uses elliptical mirrors. $BaSO_4$ was used as a 100% reflectance standard. Scans were performed from 2500 to 200 nm. Wavelength data were converted to electron volts and the percent reflectance data were converted to absorbance units using the Kubelka–Munk equation [14].

2.3.4. Second harmonic generation (SHG) measurements

SHG of a powdered sample of Li_2ZnSnS_4 was measured using a modified Kurtz NLO system [15] with a Nd:YAG laser, as described elsewhere [16]. The response of Li_2ZnSnS_4 was compared to that of α-quartz, a typical standard for this technique.

2.3.5. Powder X-ray diffraction

Powder diffraction patterns were collected using a Panalytical X'Pert Pro MPD powder X-ray diffractometer. Data were collected from 5° to 80° 2θ with a sampling interval of 0.083556°. The scan rate used was 0.010577°/s. Samples were spun during data collection. The instrument was set to an accelerating voltage of 45 kV and a filament current of 40 mA. Copper K_α radiation with a wavelength of 1.541871 Å was used for measurements. Samples were prepared for analysis by spreading powder onto a piece of double-sided tape adhered to a glass slide placed into the aluminum sample holder.

2.3.6. Single-crystal X-ray data collection and reduction

Single-crystal X-ray diffraction data were collected on a Bruker SMART Apex 2 CCD diffractometer at room temperature. Data were collected for 20 s per frame using Mo $K\alpha$ radiation with a wavelength of 0.71073 Å and a graphite monochromator. During data collection the instrument was set to 50 kV and 30 mA. The Bruker SAINT [17] program was used for data integration. After integration, there were a total of 4751 reflections collected with 1493 unique. An empirical absorption correction was performed using the SADABS [17] program.

2.3.7. Solving and refining the crystal structure

The data were analyzed using the SHELXTL-PC package [18]. Based on the suspected Laue symmetry and systematic absences, two space groups seemed possible: noncentrosymmetric $Pmn2_1$ (No. 31) and centrosymmetric $Pmmn$ (No. 51). The intensity statistic, $|E^*E-1| = 0.846$, favored neither option. Li_2ZnSnS_4 was predicted to be a homeotype of the hexagonal mineral wurtzite (ZnS); therefore the noncentrosymmetric orthorhombic space group $Pmn2_1$ was selected. The structure was initially determined in this space group with the tin and zinc sites discovered by Patterson methods. Other atoms were located by

difference-Fourier methods and chemical reasoning. The resulting structure model produced an *R*-index of 3.21%. While the model appeared fine statistically, the structure had serious anomalies. In the difference-Fourier map, a spherical $3e^-$ negative feature occupied one potential lithium site, while the second lithium site possessed an odd static disorder between lithium and zinc ions. This disorder problem was particularly alarming, for it represented a random scrambling of lithium and zinc ions at that site throughout the crystal structure. While this type of disorder has been observed in other compounds [19,20], in this case it represents a major violation of Pauling's electrostatic valency principle, since in this model the disorder could result in a sulfur anion with one lithium ion, two zinc ions and one tin ion in its immediate coordination sphere. For these reasons, the noncentrosymmetric option was abandoned and the centrosymmetric option was evaluated.

The structure was redetermined in space group *Pmmn*, resulting in a model that converged with an *R*-index of 4.38%. Both lithium ions were located and refined, but the Li/Zn disorder remained. In this case, the sulfur tetrahedra showed static disorder, which was considered highly unlikely. After much thought, the centrosymmetric model was also abandoned.

Finally, it was determined that the data were actually from a pseudo-merohedrally twinned crystal, which mimicked disorder. In a pseudo-merohedral twin, the twin operator belongs to a higher crystal system than the structure [21]. In this case, the metric symmetry possessed an additional 2-fold axis, which allowed a monoclinic structure to mimic orthorhombic symmetry. Therefore, the crystal consists of multiple ordered domains related by 2-fold axes. The orientation of the two ordered domains can be found in Fig. 2. The appearance of the 50/50 Li/Zn disorder

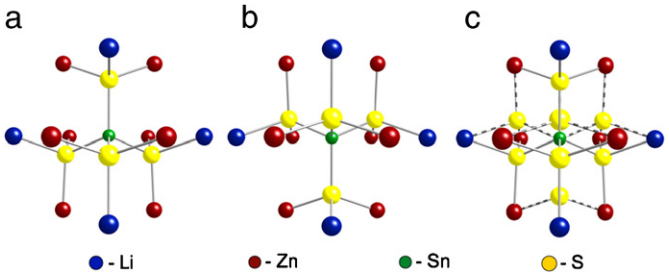

Fig. 2. The orientation of the twin components is shown separately (a) and (b) and then combined in (c).

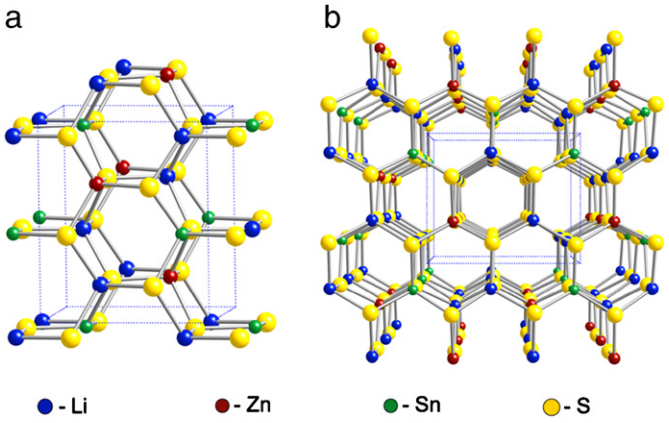

Fig. 3. (a) The crystal structure of Li_2ZnSnS_4 viewed slightly skewed from the *a*-axis, in order to better visualize the cation arrangement in the structure (b) and the expanded view directly down the *a*-axis.

Table 1
Crystallographic data and experimental details for Li_2ZnSnS_4

Empirical formula	Li_2ZnSnS_4
Formula weight	326.20
Temperature	293(2) K
Wavelength	0.71073 Å
Space group	*Pn*
Unit cell dimensions	$a = 6.3728(13)$ Å $b = 6.7286(13)$ Å $c = 7.9621(16)$ Å $\alpha = 90^\circ$ $\beta = 90.00(3)^\circ$ $\gamma = 90.00^\circ$
Volume	341.42 (12) $Å^3$
Z, calculated density	2, 3.173 Mg/m^3
Absorption coefficient	4.859 mm^{-1}
F(000)	292
Reflections collected/unique	4751/1493
Data/restraints/parameters	1493/2/64
Completeness to theta = 27.06	100.0%
Goodness of fit	1.058
Final *R* indices [$I > 2$sigma(I)]	$R1 = 0.0161$, $wR^2 = 0.0363$
R indices (all data)	$R1 = 0.0168$, $wR^2 = 0.0368$

Table 2
Atomic coordinates and equivalent isotropic displacement parameters ($Å^2 \times 10^3$) for Li_2ZnSnS_4

	x	*y*	*z*	*U*(eq)[a]
Li(1)	0.6070(80)	0.1640(11)	0.5800(30)	7(3)
Li(2)	0.1280(80)	0.3390(30)	0.8200(50)	61(9)
Zn(1)	0.1111(4)	0.3263(1)	0.3174(3)	15(1)
Sn(1)	0.6113(3)	0.1726(1)	0.0658(2)	13(1)
S(1)	0.9883(9)	0.1815(3)	0.0711(13)	16(1)
S(2)	0.9890(9)	0.1618(3)	0.5644(12)	14(1)
S(3)	0.4925(15)	0.3393(5)	0.8260(11)	16(1)
S(4)	0.4785(14)	0.3303(5)	0.3181(11)	13(1)

[a] *U*(eq) is defined as one-third of the trace of the orthogonalized U_{ij} tensor.

in the orthorhombic models shows that the crystal is a perfect twin.

The crystal structure was re-evaluated in space group *Pn* (no. 7, a subgroup of the predicted $Pmn2_1$). The twin law, 1 0 0 0 −1 0 0 0 −1, was added to the instruction file. The lithium ions were refined isotropically. No anomalous features were present in the structure model, Fig. 3. The scattering factors for the lithium and zinc ions were used instead of those for the neutral atoms. The final model was refined with $R1 = 1.68\%$ and $wR^2 = 3.68\%$ (all data). The largest positive and negative features remaining on the difference-Fourier map were 0.56 and −0.35 $e/Å^3$, respectively. Crystallographic data and experimental details of the data collection are listed in Table 1, final atomic coordinates and equivalent displacement parameters are in Table 2 and selected bond distances and angles are given in Table 3.

3. Results and discussion

The synthesis of quaternary DLS materials is relatively straightforward; however, obtaining a *phase-pure* product can often be problematic. This is due to the possibility of phase segregation resulting in stable binary products such as wurtzite (ZnS) [11,12] and herzenbergite (SnS) [22,23]. Initial high-temperature syntheses at 825, 775 and 760 °C of Li_2ZnSnS_4 did not result in a phase-pure product. Secondary phases of ZnS [24] and SnS [25] were detected by powder X-ray diffraction with a few very small peaks that could not be attributed to any known phase.

Table 3
Selected bond distances (Å) and angles (°) found in Li_2ZnSnS_4

Li(1)–S(1)	2.43(6)	S(1)–Li(1)–S(2)	108.1(12)
Li(1)–S(2)	2.431(18)	S(1)–Li(1)–S(3)	110.14(13)
Li(1)–S(3)	2.39(2)	S(1)–Li(1)–S(4)	106.4(14)
Li(1)–S(4)	2.52(2)	S(2)–Li(1)–S(3)	114.3(13)
		S(2)–Li(1)–S(4)	106.3(12)
		S(3)–Li(1)–S(4)	110.9(12)
Li(2)–S(1)	2.46(5)	S(1)–Li(2)–S(2)	110.1(18)
Li(2)–S(2)	2.45(4)	S(1)–Li(2)–S(3)	113.0(2)
Li(2)–S(3)	2.36(7)	S(1)–Li(2)–S(4)	108.0(2)
Li(2)–S(4)	2.45(3)	S(2)–Li(2)–S(3)	109.0(2)
		S(2)–Li(2)–S(4)	105.2(18)
		S(3)–Li(2)–S(4)	111.4(16)
Zn(1)–S(1)	2.400(9)	S(1)–Zn(1)–S(2)	113.1(2)
Zn(1)–S(2)	2.320(9)	S(1)–Zn(1)–S(3)	107.6(3)
Zn(1)–S(3)	2.351(4)	S(1)–Zn(1)–S(4)	108.9(3)
Zn(1)–S(4)	2.335(9)	S(2)–Zn(1)–S(3)	108.8(3)
		S(2)–Zn(1)–S(4)	109.8(3)
		S(3)–Zn(1)–S(4)	108.6(3)
Sn(1)–S(1)	2.395(2)	S(1)–Sn(1)–S(2)	110.15(14)
Sn(1)–S(2)	2.406(6)	S(1)–Sn(1)–S(3)	111.0(2)
Sn(1)–S(3)	2.349(9)	S(1)–Sn(1)–S(4)	106.7(2)
Sn(1)–S(4)	2.415(9)	S(2)–Sn(1)–S(3)	109.2(4)
		S(2)–Sn(1)–S(4)	109.0(4)
		S(3)–Sn(1)–S(4)	110.66(14)

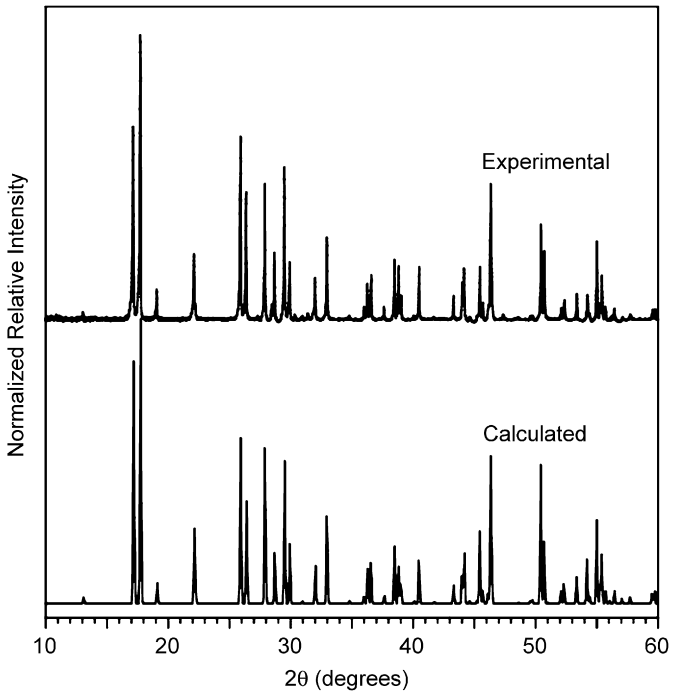

Fig. 4. A comparison of the diffractogram of an experimentally obtained sample of Li_2ZnSnS_4 compared to that calculated from the X-ray structure solution.

Lowering the reaction temperature to 700 °C resulted in a more phase-pure sample, with smaller amounts of the ZnS and SnS components. Additionally, the phase purity could be increased slightly by carrying out the reaction with a slight excess of Li_2S, see Fig. 4. This is not unexpected, as the Li_2S is highly volatile and small amounts can escape from the graphite crucible and deposit on the cold end of the fused-silica tube.

Thermal analysis of the product shows an endothermic event occurring at 919 °C, which we believe to be the melting point of Li_2ZnSnS_4, see Fig. 5. Upon cooling there is a corresponding exothermic event at 904 °C which can be attributed to the

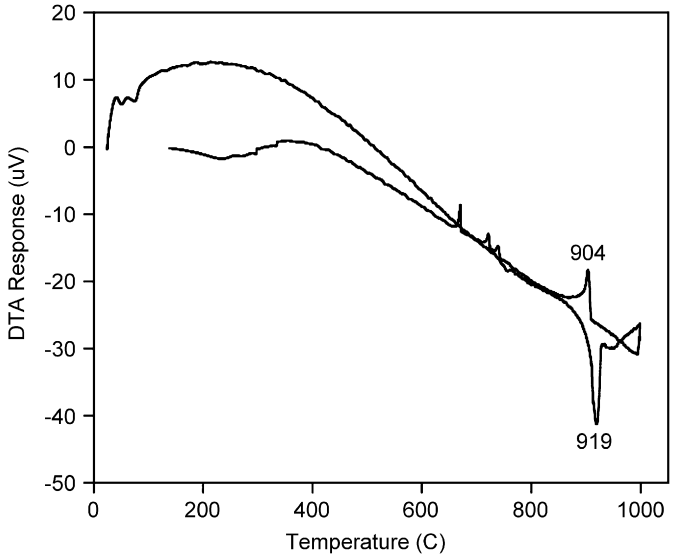

Fig. 5. Differential thermal analysis of a sample obtained for Li_2ZnSnS_4.

recrystallization of the material. The small SnS impurity, which was indicated by powder X-ray diffraction, may be showing up as the shoulder on these events, since SnS has a melting point of 880 °C [26]. Events due to ZnS are not present because it melts at 1700 °C [26], out of the range of this experiment. We suppose that Li_2ZnSnS_4 partially decomposes after melting, yielding increased amounts of the binary impurity phases; however, powder diffraction of the DTA residue was complicated by side reactions with the sample tube, despite careful carbon coating to prevent such reactions. Therefore, the several exothermic events upon cooling have not been assigned, as they are likely due to side reactions with the fused-silica ampoule. Examination of the ampoule after analysis showed glass attack as the ampoule became discolored and brittle and the sample appeared oxidized, with some white color present.

Diffuse reflectance UV/Vis/NIR spectroscopy was performed on the most phase-pure sample. The spectrum can be found in Fig. 6. The bandgap of Li_2ZnSnS_4 was estimated to be 2.87 eV from these data. In agreement with the powder X-ray diffraction results, the optical absorption spectrum suggests the presence of small impurities. The shoulder on the higher energy side of the band edge should be due to ZnS, which has a bandgap of 3.8–3.9 eV [27]. SnS has a lower bandgap, approximately 1.1 eV [28], and is likely responsible for the tail on the band edge at lower energies.

Second harmonic generation, a frequency doubling effect, requires the absence of an inversion center in a compound. DLS compounds are inherently noncentrosymmetric, which makes them ideal candidates for SHG. Interestingly, even though Li_2ZnSnS_4 is noncentrosymmetric, it did not exhibit any SHG response. One possible reason why SHG was not observed could be that the signal is very weak and/or suppressed by the presence of impurities. Additionally, we believe that this may be due to the nature of the perfect twin, although we could not find any precedent for this phenomenon in the literature. Further studies on the suppression of the second harmonic response are in progress [29].

Known quaternary DLS normally crystallize in one of three space groups: $I\text{-}42m$, $Pmn2_1$, or $Pna2_1$, with stannite and wurtz-stannite structure types. The $I\text{-}42m$ structure can be derived from that of cubic diamond, while $Pmn2_1$ and $Pna2_1$ are superstructures of hexagonal diamond. The name "wurtz-stannite" was originally applied to the predicted, disordered wurtzite structures [30],

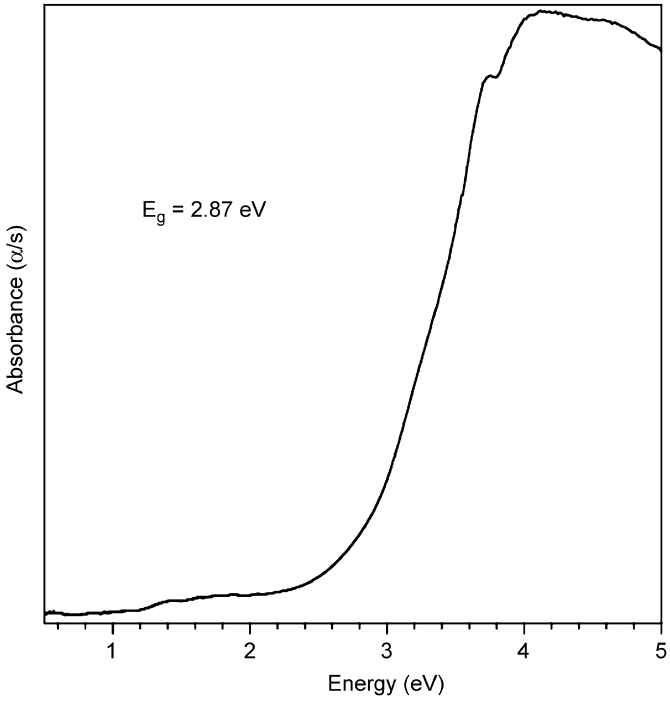

Fig. 6. Diffuse reflectance UV/Vis/NIR spectrum of Li_2ZnSnS_4.

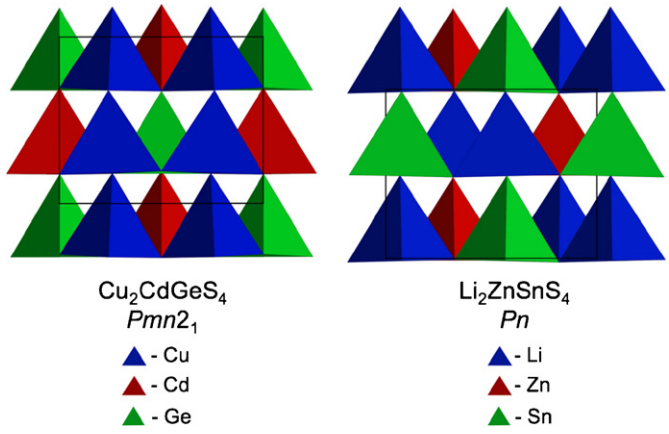

Fig. 7. Polyhedral representation of (a) Cu_2CdGeS_4 and (b) Li_2ZnSnS_4 viewed down the *b*-axis to show the difference in the ordering of the cations.

although no mineral was found to posses this structure until the discovery of orickite ($CuFeS_2$ doped with $<0.05\%$ K^+, Na^+) [31]. Li_2ZnSnS_4 crystallizes in the monoclinic space group *Pn*, which is a subgroup of $Pmn2_1$.

The loss of symmetry, resulting in the crystallization in *Pn*, cannot be attributed to deviations from perfect tetrahedral geometry; however, it can be explained by a variation in the ordering of the cations. To determine if there was a difference in the cation ordering, the structure of Li_2ZnSnS_4 was compared to that of Cu_2CdGeS_4 [3], with space group $Pmn2_1$. A difference exists in the cation ordering down each crystallographic axis. As an example, the difference in cation ordering down the *b*-axis is apparent in Fig. 7. Cu_2CdGeS_4 has two rows of cations. The first row consists of alternating Cd and Ge atoms, while the second row contains exclusively lithium atoms. The lithium atoms in Li_2ZnSnS_4 are split between the rows, with one row containing Zn and Li and the other containing Sn and Li. Another possible space group for quaternary DLS is $Pna2_1$. This option is related to $Pmn2_1$, but a difference in the ordering of the cations leads to the doubling of one unit cell edge.

All ions in Li_2ZnSnS_4 possess tetrahedral environments, with each sulfide anion being surrounded by one zinc, one tin (IV) and two lithium cations as shown in Fig. 3. The Sn–S bond distances range from 2.349(9) to 2.415(9) Å (average = 2.39(1) Å), with S–Sn–S angles from 106.7(2) to 111.1(2)°. These distances compare favorably with the Sn–S distance found in stannite (Cu_2FeSnS_4), which is 2.393(3) Å [32]. The Zn–S bond distances range from 2.320(9) to 2.400(9) Å (average = 2.35(2) Å), with angles ranging from 107.6(3) to 113.1(2)°. The Zn–S bonds in this compound are slightly larger than the 2.283 Å bond lengths found in the related quaternary compound Cu_2ZnGeS_4 [33], but are very similar to the bond distances of 2.340 Å in ZnS [11]. The distance between divalent cations in Li_2ZnSnS_4 is 5.609 Å, which is significantly longer than 3.803 Å, as found in wurtzite [11]. The LiS_4 tetrahedra are the least perfect in the structure. The Li–S bond distances range from 2.36(7) to 2.52(2) Å (average = 2.4(1) Å), with S–Li–S angles of 105.2(18)–114.3(13)°. The bond distances for Li–S in this compound agree with a value of 2.4534(9) Å for the bond lengths in the quaternary compound Li_2PbGeS_4 [34].

4. Conclusions

The structure of the new diamond-like semiconductor Li_2ZnSnS_4 has been solved from a pseudo-merohedrally twinned crystal. This twin model may explain some of the anomalies found in the related compound Li_2CdSnS_4 [35]. Future studies will investigate whether this twinning may be responsible for the lack of any SHG response exhibited by this compound. Future work will also include the use of this compound as a host structure for interesting electronic, magnetic and photovoltaic materials.

Supporting Information

Further details of the crystal structure investigation may be obtained from Fachinformationszentrum Karlsruhe, 76344 Eggenstein-Leopoldshafen, Germany (Fax: (+49)7247-808-666; E-mail: crysdata(at)fiz-karlsruhe.de, http://www.fiz-karlsruhe.de/request_for_deposited_data.html). CSD number 419595.

Acknowledgments

We thank Duquesne University's Bayer School of Natural and Environmental Sciences, NSF-DUE-05-11444 and NSF-CRIF-02-34872 for equipment. This work was supported by the National Science Foundation (Career Award, DMR-06-45304). BML and CHL thank the NSF Summer Program in Solid-State & Materials Chemistry (DMR-03-03450) for funding. We would also like to thank Professor P. Shiv Halasyamani for fruitful discussions and performing SHG measurements.

References

[1] N.A. Goryunova, in: J.C. Anderson (Ed.), The Chemistry of Diamond-like Semiconductors, The M.I.T. Press, Cambridge, 1965.
[2] E. Parthé, Crystal Chemistry of Tetrahedral Structures, Gordon and Breach Science Publishers, New York, 1964.
[3] E. Parthé, K. Yvon, R.H. Deitch, Acta Crystallogr. B 25 (1969) 1164–1174.
[4] D.M. Schleich, A. Wold, Mater. Res. Bull. 12 (1977) 111–114.
[5] M. Quintero, A. Barreto, P. Grima, R. Tovar, E. Quintero, G.S. Porras, J. Ruiz, J.C. Woolley, G. Lamarche, A.M. Lamarche, Mater. Res. Bull. 34 (1999) 2263–2270.
[6] A. Goetzberger, C. Hebling, H. Schock, Mater. Sci. Eng. 40 (2003) 1–46.
[7] M.C. Ohmer, R. Pandey, MRS Bull. 23 (1998) 16–20.
[8] G.C. Catella, D. Burlage, MRS Bull. 23 (1998) 28–36.

[9] G.E. Davidyuk, O.V. Parasyuk, S.A. Semenyuk, Ya.E. Romanyuk, Inorg. Mater. 39 (2003) 919–923.
[10] S.J. Pearton, C.R. Abernathy, D.P. Norton, A.F. Hebard, Y.D. Park, L.A. Boatner, J.D. Budai, Mater. Sci. Eng. 40 (2003) 137–168.
[11] G. Aminoff, Z. Kristallogr. Krist. 58 (1923) 203–219.
[12] H.T. Evans Jr., E.T. McKnight, Am. Mineral. 44 (1959) 1210–1218.
[13] H. Hahn, G. Frank, W. Klingler, A.D. Meyer, G. Stoerger, Z. Anorg. Allg. Chem. 271 (1953) 153–170.
[14] P. Kubelka, F. Munk, Z. Tech. Phys. 12 (1931) 593–601.
[15] S.K. Kurtz, T.T. Perry, J. Appl. Phys. 39 (1968) 3798–3813.
[16] K.M. Ok, N.S. Bhuvanesh, P.S. Halasyamani, Inorg. Chem. 40 (2001) 1978–1980.
[17] SAINT and SADABS are part of the Apex 2 software package v2.1-4 Program for Data Collection and Reduction on Bruker AXS CCD Area Detector Systems, Bruker Analytical X-ray Systems, Inc., Madison, WI, 2005.
[18] SHELXTL-PC release 6.14, Bruker AXS, Madison, WI, 2007.
[19] B. Deng, G.H. Chan, F.Q. Huang, D.L. Gray, D.E. Ellis, R.P. Van Duyne, J.A. Ibers, J. Solid State Chem. 180 (2007) 759–764.
[20] D. Schmitz, W. Bronger, Z. Anorg. Allgem. Chem. 553 (1987) 248–260.
[21] R. Herbst-Irmer, in: P. Müller (Ed.), Crystal Structure Refinement: A Crystallographer's Guide to SHELLXL, Oxford University Press, New York, 2006.
[22] S. Del Bucchia, J.C. Jumas, M. Maurin, Acta Crystallogr. B 37 (1981) 1903–1905.
[23] L. Guen, W.S. Glaunsinger, A. Wold, Mater. Res. Bull. 14 (1979) 463–467.
[24] E.A. Jumpertz, Z. Elektrochem. 59 (1955) 419–425.
[25] S.B. Badachhape, A. Goswami, J. Phys. Soc. Jpn. (Suppl. 17) (1962) 251–253.
[26] D.R. Lide (Ed.), Handbook of Chemistry and Physics, CRC Press, New York, 2003.
[27] O. Madelung, M. Schulz (Eds.), Numerical Data and Functional Relationships in Science and Technology. New Series. Group III: Crystal and Solid State Physics. Semiconductors. Supplements and Extensions to Volume III/17. Intrinsic Properties of Group IV Elements and III–V, II–VI and I–VII Compounds, Vol. 22a, Springer, Berlin, 1982.
[28] A.M. Elkorashy, Chemtronics 1 (1986) 76–79.
[29] J.W. Lekse, J.A. Aitken, P.S. Halasyamani, S. work in progress.
[30] W. Schäfer, R. Nitsche, Mater. Res. Bull. 9 (1974) 645–654.
[31] R.C. Erd, G.K. Czamanske, Am. Mineral. 68 (1983) 245–254.
[32] J. Llanos, M. Tapia, C. Mujica, J. Oro-Sole, P. Gomez-Romero, Bol. Soc. Chil. Quim. 45 (2000) 605–609.
[33] A.F. Moodie, H.J. Whitfield, Acta Crystallogr. B B42 (1986) 236–247.
[34] J.A. Aitken, P. Larson, S.D. Mahanti, M.G. Kanatzidis, Chem. Mater. 13 (2001) 4714–4721.
[35] M.S. Devi, K. Vidyasagar, J. Chem. Soc., Dalton Trans. (2002) 2092–2096.